

Short-term variability of the Mediterranean in- and out-flows

Claude Millot
Laboratoire d'Océanographie Physique Biogéochimique
Antenne de La Seyne/mer, BP 330, F-83150
cmillot@ifremer.fr

Abstract

A re-analysis of CTD profiles collected in the Strait of Gibraltar during the 1985-1986 Gibraltar Experiment shows that a large variability can occur, within a 10-day interval, in the nature of the Atlantic Water found in the sill surroundings and expected to flow into the Mediterranean Sea, and in the set of Mediterranean Waters outflowing from the sea. Since both strongly mix together within the strait, the Mediterranean outflow in the Atlantic Ocean can display a tremendous short-term variability. Specifying any nominal characteristic for the outflow all its way downstream, a fortiori any nominal characteristic for the various veins into which it is split, thus needs monitoring the whole water column within the strait.

Introduction

Because evaporation exceeds precipitation and river run-off over the Mediterranean Sea, a surface inflow of fresh Atlantic Water (AW; salinity $S \sim 36$) and a deep outflow of salty Mediterranean Water (MW; $S \sim 38$) occur through the Strait of Gibraltar (e.g. Lacombe and Richez, 1982). Mainly due to the large amplitude of the internal tide and to intense non-linear processes, both the inflow and the outflow strongly mix together (e.g. Wesson and Gregg, 1994), in particular in the Camarinal Sill South surroundings (near $5^{\circ}45'W$, sill ~ 300 m, Fig. 1).

Up to nowadays, attempts have been made to better understand both the composition of the outflow and the processes that led waters found at ~ 1000 m in the western Alboran subbasin to be raised up to the sill. Because they can easily be recognised on nearly all θ - S (θ : potential temperature) diagrams within the western basin of the sea and within the Alboran in particular, the sole components of the outflow have generally been considered (e.g. Baringer and Price, 1999) to be the relatively warm and salty Levantine Intermediate Water (LIW), the intermediate water formed in the eastern basin, and the relatively fresh and cool Western Mediterranean Deep Water (WMDW),

the deep water formed in the western basin. The hypothesis put forward by Stommel et al. (1973) that the rapid outflow of LIW was able, through the Bernoulli effect, to suck WMDW up to the sill is also generally thought to be supported by in situ data (e.g. Kinder and Parrilla, 1987). Finally, it is also generally assumed (following Parrilla et al., 1989) that these two Mediterranean Waters (MWs) are mixed near $6^{\circ}05'W$, hence producing a homogeneous outflow that is then split into veins, due to its cascading along different paths and to different mixing conditions with the Atlantic Water (AW). Note that the assumption of an homogeneous outflow at the strait outlet is used in most of the recent data analyses (e.g. Ambar et al., 2002), laboratory experiments (e.g. Davies et al., 2002) and numerical simulations, be the latest dedicated to the general circulation at ocean scale (e.g. Wu et al., 2007), to the exchanges through the strait (e.g. Sannino et al., 2002), or to the outflow itself (e.g. Serra and Ambar, 2002).

Most of these thoughts were inferred from analyses of a very valuable set of data, in particular CTD profiles, collected in 1985-1986 during the Gibraltar Experiment (Bryden and Kinder, 1991). However, better considering the circulation of the MWs within the whole sea and the Alboran subbasin in particular, and taking into account 2003-2007 time series from two CTDs moored (CIESM Hydro-Changes Programme) at the sill (270 m) and on the Moroccan shelf (~80 m), a re-analysis of the same data set leads to markedly different conclusions (Millot, submitted, www.ifremer.fr/lobtln) that are more or less illustrated hereafter. It is clear that the Winter Intermediate Water (WIW), the intermediate water that is formed from the AW cooling in the north of the western basin and lies above LIW, and the Tyrrhenian Dense Water (TDW), the water that results from the cascading of the deep eastern waters into the western basin and that lies between LIW and WMDW, are major components of the outflow too. In the western Alboran, it also appears that the necessary velocity increase of the outflow and the Coriolis effect induce a marked tilting up of the intermediate-deep MWs interface that can bring the deep MWs up to the southern part of the sill. There, the tilting makes all MWs mixing individually with AW, hence leading to an outflow that is markedly heterogeneous horizontally. The widening of the strait after the sill and the necessary velocity decrease of the outflow make isopycnals tilting down and the outflow becoming heterogeneous vertically, hence forming veins as soon as $\sim 6^{\circ}15'W$. Together with decadal changes in the composition of the outflow (Millot et al., 2006) and with marked seasonality and interannual trends of the inflow's salinity (Millot, 2007), the re-analysis of the Gibraltar Experiment data set we have undertaken thus already provided us with another understanding of both the inflow and outflow variability at sub inertial and longer time scales.

We focus hereafter on the short-term variability of both the inflow and the outflow, aiming to show that, if the simplified assumption of an homogeneous outflow has to be made for practical reasons, its characteristics are much variable in time than previously expected. The data set is presented in section 2 and analysed in section 3 before concluding in section 4.

2. The data set

Whatever the analyses made and the results obtained either in the previous decades by numerous authors or recently by ourselves, the major interest of the 1985-1986 Gibraltar Experiment data set is that numerous cross-strait / north-south CTD transects were repeated several times using relatively small space intervals (2-3 nautical miles (nm) in general, sometimes less) during several campaigns referred to as "LYNCH-702-86" (Nov. 1985), "GIB1" (Mar.-Apr. 1986) and "GIB2" (Sep.-Oct. 1986) in the MEDATLAS database (MEDAR group, 2002). Another interest of these campaigns is that, even though the bathymetry can be relatively steep, most of the profiles were made down to a few metres above the bottom, which guarantees that no significant amount of any MWs was missed. The GIB1 and GIB2 campaigns are interesting because, even though transects were not repeated, they covered the whole study area, in particular the eastern Alboran and the strait itself, within one week and while the dynamical regime was relatively stable; we analysed most of the profiles between $4^{\circ}30'W$ and $6^{\circ}15'W$ (Millot, submitted) and consider only some of them hereafter. The LYNCH-702-86 campaign is interesting for the purpose of the present paper because, first and even though it focused on the strait itself only, transects were repeated several times within two weeks in between and at the longitudes ($\sim 5^{\circ}15'W$ and $\sim 6^{\circ}05'W$) that were considered to be its entrance and outlet (for the MWs). This campaign is also interesting because marked changes in the hydrodynamical regime that are detailed hereafter occurred meanwhile.

Bray et al. (1995) previously made a statistical analysis of the whole Gibraltar Experiment data set. They did not differentiate the various MWs and indicated that AW was in fact composed of North Atlantic Central Water (NACW, $\theta = 12-14^{\circ}C$, $S = 35.5-36.0$ in the study area), found during all campaigns and overlaid by a modified form of NACW that was named Surface Atlantic Water (SAW, $\theta = 16-22^{\circ}C$, $S = 36.0-36.5$ in the study area). Therefore, they interpreted the θ and S distributions within the strait as a mixture of these three principal water types and inferred typical percentages for an upper layer, an interface layer and a lower layer, as well as seasonal and east-west variations. Such general features are far from being supported by a more detailed analysis of the available data set, in particular the LYNCH-702-86 one (1-17 Nov. 1985).

Transects at several nominal longitudes ($6^{\circ}05'W$, $5^{\circ}50'W$, $5^{\circ}40'W$, $5^{\circ}30'W$, $5^{\circ}15'W$; more accurate locations can be found in e.g. Bray et al. (1995)) were repeated several times in an order that makes them more or less convenient for our purpose. The $5^{\circ}15'W$ transect was performed on Nov. 6-7 and 10-11, which appears to be a too short interval, furthermore data from the $5^{\circ}30'W$ transect, performed on Nov. 5, 9-10 and 16-17 show that major changes occurred in the composition of the MWs outflow between the two last surveys; information provided by the $5^{\circ}30'W$ and $5^{\circ}40'W$ transects are roughly similar. The $6^{\circ}05'W$ transect was suitably covered on Nov. 1-2 and 15, as well as the $5^{\circ}50'W$ transect covered on Nov. 2-3 and 13-14, which is a particularly interesting transect since located just west from the sill. We thus decided to present only the data collected about 10 days apart (Nov. 1-5 vs. Nov. 15-17) at $6^{\circ}05'W$ (where maximum depths are ~ 400 m), $5^{\circ}50'W$ (~ 400 m) and $5^{\circ}30'W$ (~ 950 m). Note that at all longitudes

and at both the beginning and the end of the campaign, the transects were in fact performed twice at roughly similar locations, which guarantees the significance of the collected data that are all considered at the available 1-dbar sampling interval. Transects on Nov. 1-5 (resp. 15-17) are thus referred to as LYNCH1+2 (resp. LYNCH3+4) in the figures and named L12 and L34 in the text.

3. The data analysis

Overall, the θ -S diagrams in Figure 2 show that, for what concerns AW mainly, L12 (blue), GIB1 (grey) and GIB2 (grey) display relatively similar features in the whole study area; as confirmed by other historical data sets, it is clear that L34 (red) represents an abnormal situation in the inflowing AW layer. Normal general features there are, in particular, the S minimum (35.8-35.9) at the base of the NACW layer that rises, according to the L12 data, from 200-280 m at 6°05'W to 200-230 m at 5°50'W, while the NACW characteristics are not seasonally dependent (e.g. GIB1 vs. GIB2, not clear in the figure). Eastward from the sill longitude (~5°45'W), the S minimum is less clearly defined and the inflow's S displays a marked seasonal variability (Millot, 2007). Only the SAW characteristics during fall are clearly displayed in the figure, those during spring (GIB1) being in particular a θ maximum of ~16 °C (Millot, 2008-submitted). The other major information from Fig. 2 is that the MWs mixed only with NACW during L12 in the whole area, while during L34 they mixed with both SAW and a markedly modified NACW at 6°05'W, with SAW only at both 5°50'W and 5°30'W since NACW was totally absent there. This leads to dramatically different AW-MWs mixing lines.

At 6°05'W (Fig. 2a), SAW was present during all campaigns while NACW was relatively rare during L34 performed ~10 days after L12 and ~6 months (resp. ~1 year) before GIB1 (resp. GIB2). Additionally, mixing with the MWs was significant at all places in a 250-m surface layer during L34 while it sometimes did not reach such a layer during L12. Differences between L34 and L12 in particular are even more dramatic at 5°50'W (Fig. 2b) since mixing with the MWs was significant at all places in a 100-m surface layer during L34 while it never reached such a layer during L12. Similar observations can be made at 5°30'W and for a 50-m surface layer (Fig. 2c). It can be concluded from the L12 vs. L34 differences in Fig. 2 that a reduced amount of NACW in the whole study area allows the MWs to influence a thicker bottom layer.

Overall, Fig. 3 allows focusing on the AW-MWs mixing lines in the deepest part of the profiles. In addition to the differences between the slopes of the L12 (NACW-MWs) and L34 (SAW-MWs) mixing lines already shown, Fig. 3 indicates that the amount of points in the displayed ranges reduces, from east (Fig. 3c) to west (Fig. 3a), much more for L12 than for L34. Mixing of the MWs thus modified their characteristics more during L12 (with NACW) than during L34 (with SAW). This is supported by the decrease, from east to west, of the maximum density values that was larger during L12 than during L34. Additionally, and even though Fig. 3c suggests that the MWs east of the

sill were less dense during L34 than during L12, maximum densities west of the sill (Fig. 3a,b) were larger during L34 than during L12. The slope of the AW-MWs mixing line during both L12 and L34 evolves from east to west according to the fact that more and more mixed relatively warm and salty MWs mix with less and less mixed relatively cool and fresh NACW.

More information about the composition of the MWs outflow while still relatively unmixed with AW, be it NACW or SAW, and about its changes from L12 to L34 can be inferred from Fig. 4c. Because θ -S diagrams there are relatively complex, only three representative profiles, selected in the northern, central and southern parts of the Alboran are plotted for each transect with one out of six data. Profiles in the south (S) indicate a straight/direct mixing line between either WMDW or the densest TDW and AW. Profiles in the centre (C) are the less straight because they mainly indicate the WIW and/or LIW cores while profiles in the north (N) indicate AW-MWs mixing lines along the continental slope. As shown by the largest densities for each of the profiles (black S, C, N), maximum values are encountered in the southern and central parts of the subbasin (see Millot, submitted, for more details).

Figure 4c shows that, as compared with the GIB1 and GIB2 data, the WIW amount during both L12 and L34 was relatively reduced. For the other MWs, L12 profiles were more classic and more similar to the GIB1-GIB2 ones than the L34 profiles that indicated relatively mixed, hence not very dense, MWs: L34 thus represents an abnormal situation also for the MWs outflow as depicted at $5^{\circ}30'W$. The situation reversed at both $5^{\circ}50'W$ (Fig. 4b) and $6^{\circ}05'W$ (Fig. 4a) since the densest outflow more and more comes to be the L34 one; note from Fig. 3 that this just results from different mixing intensities along different mixing lines, maximum mixing occurring during L12 (with NACW). Also note from the indication of the 400-m levels that maximum densities are not necessarily encountered at the greatest depths, even though still in the southern and/or central parts of the strait; it is only near $6^{\circ}15'W$, which must preferentially be considered as the strait outlet, that the largest densities are definitively found along the northern slope.

3. Discussion

It is clear from Fig. 2b in particular, that dramatic change occurred in the whole surface layer of AW between the L12 and L34 surveys, hence ~ 10 days apart, with the total disappearance of NACW in the sill surroundings. It is also clear from Fig. 4c in particular, that dramatic change also occurred within the same time interval in the deeper part of the MWs layer in the western Alboran, with the replacement of all the densest MWs by more mixed, hence less dense ones.

One can hypothesise that one change directly results from the other. Assuming that the disappearance of NACW (or the relative extension of the more superficial SAW) in the inflow is the cause should lead in the Alboran to a reduced mixing of the MWs with

less dense AW, hence to a denser MWs outflow at 5°30'W. Assuming that the occurrence of less dense MWs is the cause should result in different mixing lines with NACW, not in its disappearance. Since such hypotheses are not supported by the available data, and even though we do not have any information about the transports, we are inclined to think that both changes just occurred by chance within the same time interval.

Considering that the MWs generally mix only with NACW, i.e. the deeper part of AW (Fig. 2), and assuming that lighter MWs outflow (Fig. 4c) while the NACW amount vanishes in the strait surroundings (Fig. 2a-c) leads to an easiest/thickest outflow (the black dots in Fig. 2) and a reduced mixing of the MWs with the more superficial SAW, which is consistent with all available data. Quantifying the mixing from 5°30'W to 5°50'W and to 6°05'W by the largest density values measured during the various transects leads to shifts from 29.099-29.103 kg.m⁻³ for L12 and 29.095-29.096 kg.m⁻³ for L34 (at 800-950 m near 5°30'W), to 28.92-28.96 kg.m⁻³ for L12 and 28.97-29.05 kg.m⁻³ for L34 (at 450-600 m near 5°50'W), and to 28.80-28.83 kg.m⁻³ for L12 and 28.85-29.00 kg.m⁻³ for L34 (at 380-420 m near 6°05'W). Even though the largest densities that occurred during each survey were probably not measured due to a still too coarse sampling interval, the total decrease between 5°30'W and 6°05'W, which can also be estimated from Fig. 4, was ~0.25 kg.m⁻³ during L12 and ~0.1 kg.m⁻³ during L34. Note that the decrease between 5°50'W and 6°05'W was similar for L12, GIB1 and GIB2. We can thus conclude that the marked change in the intensity of the MWs-AW mixing observed between L12 and L34 results more from the disappearance of NACW than from the change in the characteristics of the MWs outflow itself.

4. Conclusion

Thanks to very valuable CTD profiles collected during the 1985-1986 Gibraltar Experiment along a series of north-south cross-strait transects repeated several times within a 10-day interval, it was possible to emphasize the tremendously large short-term variability that can be encountered by both the inflowing AW and the outflowing MWs.

Within such a short-time interval, the supposedly ubiquitous NACW can totally disappear in the sill surroundings, AW just consisting then in a relatively superficial layer of SAW that is much less efficient than NACW in mixing with the MWs. This appears to have dramatic consequences for the characteristics of the outflow at the strait outlet, hence far downstream in the ocean. Such a short-term variability of AW must therefore be imperatively considered in addition to the seasonality and interannual trends already shown with autonomous CTDs moored in the sill surroundings (Millot, 2007).

The MWs outflow itself can encounter a relatively marked short-term variability that is also indicated by the on going monitoring with autonomous CTDs. This variability of the MWs must be imperatively considered in addition to the sub inertial (months to

years) changes already shown with these CTDs and a re-analysis of the same Gibraltar Experiment data set (Millot et al., 2006; Millot, submitted).

It is clear that specifying the characteristics of the Mediterranean outflow in the Atlantic Ocean, hence its influence at global scale, as well as understanding its dynamics while cascading and mixing with waters resident along the Iberian continental slope, needs describing, with relatively short space and time intervals, not only its composition at the strait entrance in terms of the four major MWs, but also the composition of AW (NACW vs. SAW) in the sill surroundings.

Acknowledgements: The various re-analyses we are proposing mainly illustrate the fact that good data sets have a value that is continuously increasing with time, and they emphasize the appreciation one must have for the very valuable work done by the involved crews, technicians, scientists and data managers.

References

Ambar, I., Serra, N., Brogueira, M.J., Cabeçadas, G., Abrantes, F., Freitas, P., Gonçalves, C., Gonzales, N., 2002. Physical, chemical and sedimentological aspects of the Mediterranean outflow off Iberia. *Deep-Sea Research II* 49, 4163-4177.

Baringer, M., Price, J., 1999. A review of the physical oceanography of the Mediterranean outflow. *Marine Geology*, 155, 63-82.

Bray, N.A., Ochoa, J., Kinder, T.H., 1995. The role of the interface in exchange through the Strait of Gibraltar. *Journal of Geophysical Research*, 100, C6, 10755-10776.

Bryden, H.L., Kinder, T.H., 1991. Recent progress in strait dynamics. *Reviews of Geophysics*, (Supp.), 617-631.

Kinder, T.H., Parrilla, G., 1987. Yes, some of the Mediterranean outflow does come from great depths. *Journal of Geophysical Research*, 92, C3, 2901-2906.

Lacombe, H., Richez, C., 1982. The regime of the Straits of Gibraltar. In: *Hydrodynamics of semi-enclosed seas*, J.C.J. Nihoul, editor, Elsevier, Amsterdam, 13-74.

MEDAR Group, 2002. MEDATLAS/2002 database. Mediterranean and Black Sea database of temperature salinity and bio-chemical parameters. *Climatological Atlas*. IFREMER Edition (4 CDroms).

Millot, C., 2007. Interannual salinification of the Mediterranean inflow. *Geophysical Research Letters*, 34, L21069, doi:10.1029/2007/GL031179, www.ifremer.fr/lobtln.

Millot, C., 2008. Another conception of the Mediterranean outflow. Submitted to *Progress in Oceanography*, www.ifremer.fr/lobtln.

Millot C., J. Candela, J.-L. Fuda and Y. Tber, 2006. Large warming and salinification of the Mediterranean outflow due to changes in its composition. *Deep-Sea Res.*, 53/4, 656-666. doi:10.1016/j.dsr.2005.12.017, www.ifremer.fr/lobtln.

Parrilla, G., Kinder, T.H., Bray, N.A., 1989. Hidrologia del Agua Mediterranea en el Estrecho de Gibraltar durante el Experimento Gibraltar (Octubre, 1985 – Octubre, 1986). In *Seminario sobre la oceanografía física del Estrecho de Gibraltar*, Madrid 24-28 Octubre, 1988, edited by J.L. Almazan, H. Bryden, T. Kinder and G. Parrilla, 95-121.

Sannino, G., Bargagli, A., Artale, V., 2002. Numerical modeling of the mean exchange through the Strait of Gibraltar. *Journal of Geophysical Research*, 107, C8, 3094, doi:10.1029/2001JC000929.

Serra, N., Ambar, I., 2002. Eddy generation in the Mediterranean Undercurrent. *Deep-Sea Research II* 49 (19), 4225–4243.

Wesson, J.C., Gregg, M.C., 1994. Mixing at Camarinal Sill in the Strait of Gibraltar. *Journal of Geophysical Research*, 99, C3, 9847-9878.

Wu, W., Danabasoglu, G., Large, W.G., 2007. On the effects of parameterized Mediterranean overflow on North Atlantic ocean circulation and climate. *Ocean Modelling*, 19 (1-2), 31-52.

Figure captions

Figure 1. The study area with the more (full lines) or less (dashed lines) informative north-south transects, and the location of Camarinal Sill South (CSS). Isobaths are the 100 m (thin), 200 m (thick), 300 m (thin), 400 m (relatively thick), 500 m (thin), 600 m (dashed) and 800 m (thin) black lines.

Figure 2. θ -S diagrams inferred from the whole set of entire CTD profiles collected near 6°05'W (a), 5°50'W (b) and 5°30'W (c) during the LYNCH-702-86 campaign on Nov. 1-5 (blue) and 15-17 (red), 1985, as well as during the GIB1 (Apr. 1986, grey) and GIB2 (Nov. 1986, grey) ones. Transects were repeated twice at the beginning (1+2) and the end (3+4) of the LYNCH campaign (available sampling interval of 1 dbar), they were performed only once during the GIB1 and GIB2 ones (available

sampling interval of 2 dbar). Black dots correspond to depths of 250 m (a), 100 m (b) and 50 m (c). Isopycnals are plotted 1.0 kg.m^{-3} apart. Acronyms are specified in the text.

Figure 3. Same as for Fig. 2 in the lowest part of the CTD profiles focusing on the MWs-AW mixing lines. Isopycnals are plotted 0.05 kg.m^{-3} apart.

Figure 4. Same as for Fig.2 in the MWs ranges. Only one profile representative of the southern (S), central (C) and northern (N) parts of the various transects are plotted with corresponding letters for each campaign (GIB1, GIB2) or survey (LYNCH 1 to 4); black letters indicate the densest value for each of the selected profiles. All available data are plotted in a) and b) while only one out of two (GIB) and one out of six (LYNCH) are plotted in c). The other profiles are just indicated by small dots. Black dots in a) and b) specify the 400-m level. Acronyms are specified in the text.

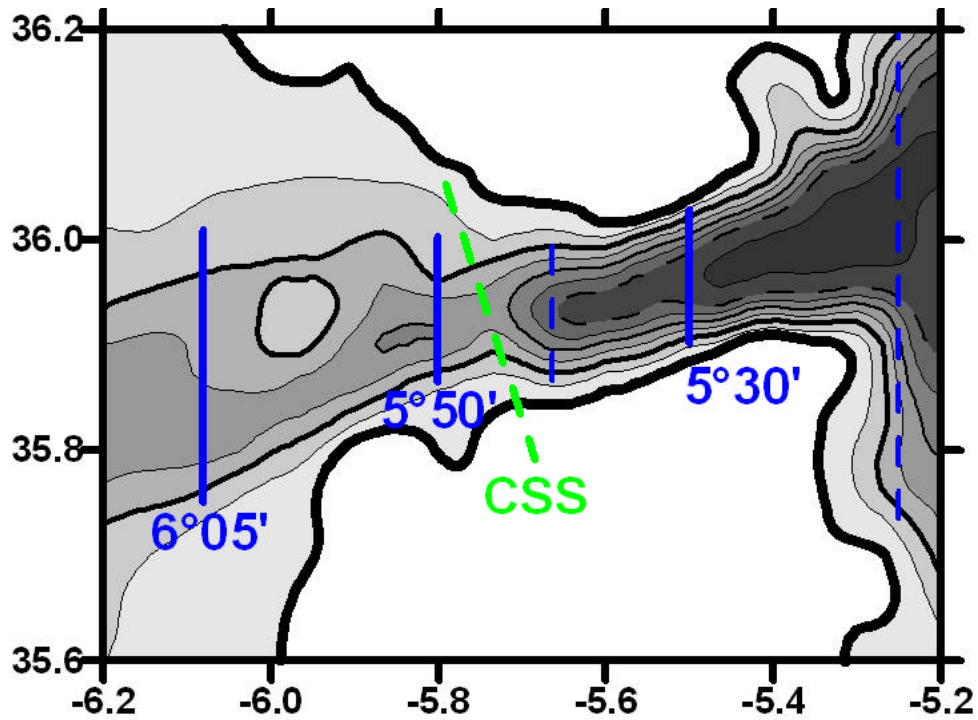


Figure 1

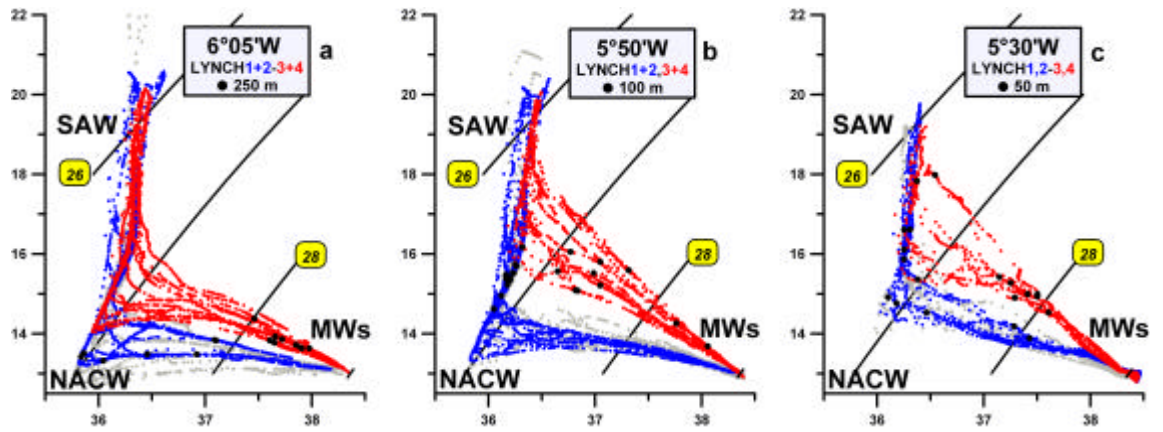


Figure 2

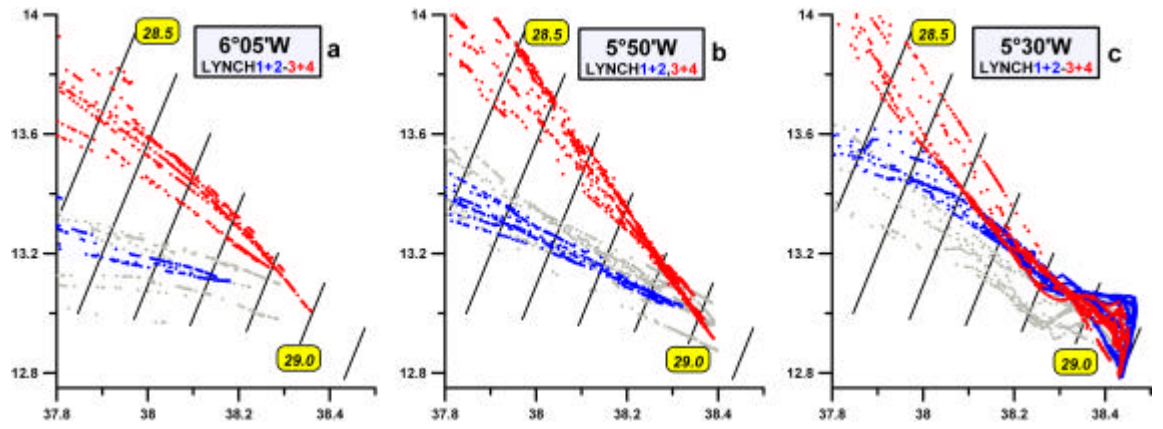


Figure 3

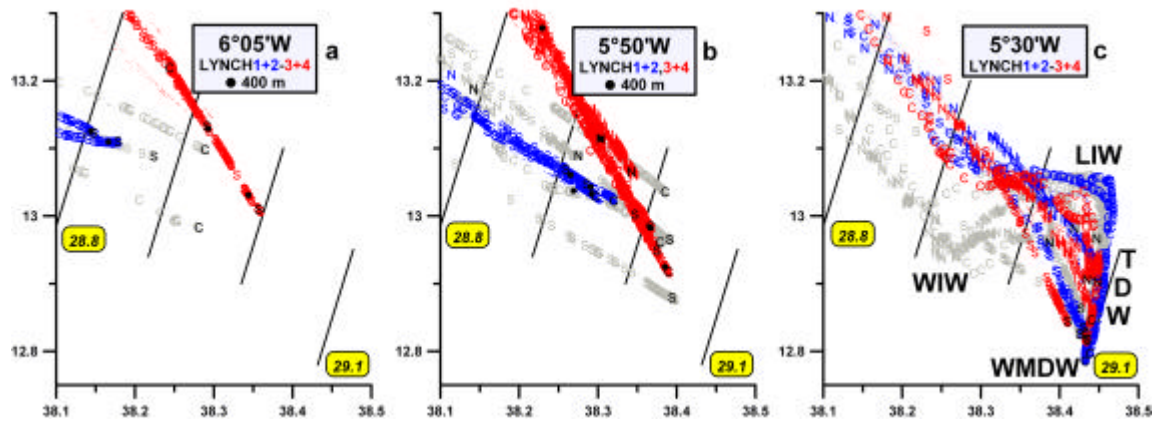


Figure 4